Wear Studies of Al$_2$O$_3$-ZrO$_2$·5CaO Composite Coatings for Tribological Applications

Abhinav[1]*, N.Krishnamurthy[2], Ranjana Jain[3]

[1]*Alliance College of Engineering and Design, Alliance University, Bangalore, India.*
[2]*VVIT,Visvesvaraya Technological University, Bangalore, India.*
[3]*KSIT,Visvesvaraya Technological University, Bangalore, India.*
*Corresponding author E-mail:abhinavtechno5@gmail.com

Abstract

A composite mixture of Metco 105 SFP, 99.9% Al$_2$O$_3$ and Metco 201 NS, ZrO$_2$.5CaO were blended in the pursuit of high hardness and improved wear resistance characteristics for tribological applications. In this context a composite mixture of alumina and calcia stabilized zirconia in 50:50 by wt. % proportion was developed, and applied over Al-6061 substrates. Atmospheric plasma spray coating technique was used to develop the coating systems. The ASTM G132 standard, a pin-on-disk tribometer was used to determine the specific wear rate at different normal loads of 5 N, 10 N and 15 N. Experimental results revealed that the top coat primarily subjected to sliding and localized abrasion and also confirmed with SEM micrograph. Sliding has mainly occurs in the plane of <111>, <200>, <220>, <311>, <222> found in the XRD analysis. Irrespective of the applied normal loads the coefficient of friction doesn't influences much in the abrasive wear studies. However, wear mechanism was found to primarily dependent on the phases and on the crystallographic structure of the material used.

Keywords: *Al$_2$O$_3$-ZrO$_2$·5CaO, roughness, porosity, microhardness, abrasive wear.*

1. Introduction

The primary source of friction between the sliding bodies mainly attributed to the resistance offered by interlocking protuberances [1].Principally, failure modes of composite coating have been identified in two ways *viz.* premature and gradual failure [2].

After extensive literature survey, it was observed that the wear of the coated samples were primarily depends on the coating microstructures, porosity, hardness, coating thickness, and operational parameters such as load, velocity, and friction [3]. Earlier investigations demonstrated that the compositions like, ZrO$_2$ + 8%Y$_2$O$_3$, ZrO$_2$ + 20% Y$_2$O$_3$, and Al$_2$O$_3$ + ZrO$_2$ coatings have superior and extended wear life against cast-iron [4,5]. It is generally found that the wear resistance of a material is closely related to its microhardness, toughness, coating defects, and the ratio of its hardness to the hardness of the abrasive [6]. In addition to hardness and toughness, the microstructure of ceramics especially grain size has an immense influence on its wear resistance [7, 8, 9,]. It has also been found that the composite phase has an important effect on the process of wear [10]. It is generally recognized that the wear of polycrystalline alumina varies significantly with mean grain size, with the wear rate, and increases rapidly with the increase in its grain size [11, 12].

Earlier investigations showed that the fine-grained ceramics have lower wear rates in comparison with that of the coarse-grained ceramics [12] .Y.Wang [13] had investigated on the abrasive wear characteristics of plasma sprayed nanostructured alumina-titania coatings (250 to 600 μm) on a mild steel substrate.His studied showed that the worn surfaces of conventional coatings exhibit grooves, plastic deformation, and microfracture features. However, the dominating mechanism of material removal of nanostructured coatings are due to grain dislodgement as found by Xu and Jahanmir [14].

As discussed above, there is not a single scientific model available currently, that can be used correctly as a basis for wear study. Different composites exhibit different wear mechanisms and wear rate. In the light of the above research gap, there is still scope for further investigation in the area of composite coatings.

In the present experimental work, an attempt has been made to develop a coating system that exhibits high hardness, less porosity, and demonstrate extended wear life when operated in an aggressive environment. The investigations are made on the coated Al-6061 substrate, which can find its commercial applications in the area of cylinder liner in light motor vehicles, scuba tank, valves, nozzles, gun barrels etc.The composite composition Al$_2$O$_3$-ZrO$_2$·5CaO taken in 50:50 by weight proportion and blended using ball mill technique. The primary objective of selecting above composition is to exploit the technical properties viz. hardness, resistance to corrosion, and resistance to abrasive wear. In our previous published work [15], present composite combination shows good resistance towards corrosion as the coating thickness increases. In the present paper, attempts were made to investigate the wear characteristics of the above-mentioned composition for the tribological applications.

2. Experimental Methodology

2.1 Selection of Material and Powder Trade Names

Al-6061 was selected as a substrate material. The selection of powder was based on thermal coefficient of expansion provided by Sulzer Metco and the trade names of different powders are shown in Table 1.

Table 1: Trade name and composition of the powder

Trade Name	Composition by wt.%
Metco 105 SFP	99.9% Al_2O_3
Metco 201 NS(top coat)	$ZrO_2.5CaO$
Metco 446 (bond coat for Al-6061)	Al25Fe7Cr5Ni
Metco 410 NS (bond coat for Al-6061)	$Al_2O_3$30(Ni20Al)

2.2 Coating Methodology

The Atmospheric plasma spray technique was used to coat different powders on the substrates. Before the coating process, the mixture of Al_2O_3 and $ZrO_2.5CaO$ in 50:50 was prepared using ball mill technique. The substrates were chemically cleaned using tetra chloride-ethylene followed by preheating to the temperature of 250±50 ℃. This process was done to minimise the thermal mismatch between substrate and bond coat. The schematic representation of a coating system for Al-6061 is shown in Figure 1. The top coat thicknesses were varied in 100, 200, and 300 µm, and hereafter called S1, S2, and S3 theoretical coating systems respectively. The thickness of the coating systems were selected for the optimization of results (wear rate). The plasma spray machine specification and spray parameters for bond coat and top coat are given in Table 2 and 3 respectively.

Top Coat (100 µm) Pure Ceramic ($ZrO_2.5CaO+Al_2O_3$)	Top Coat (200 µm) Pure Ceramic ($ZrO_2.5CaO+Al_2O_3$)	Top Coat (300 µm) Pure Ceramic ($ZrO_2.5CaO+Al_2O_3$)
Bond Coat 2(50 µm) (Cermet) $Al_2O_3$30(Ni20Al)	Bond Coat 2(50 µm) (Cermet) $Al_2O_3$30(Ni20Al)	Bond Coat 2(50 µm) (Cermet) $Al_2O_3$30(Ni20Al)
Bond Coat 1 (50 µm) Metallic Powder Al25Fe7Cr5Ni	Bond Coat 1 (50 µm) Metallic Powder Al25Fe7Cr5Ni	Bond Coat 1 (50 µm) Metallic Powder Al25Fe7Cr5Ni
Substrate (Al-6061)	Substrate (Al-6061)	Substrate (Al-6061)

Fig.1: The schematic representation of coating system applied on Al-6061.

Table 2: Air Plasma machine Specification

Specifications	Parameters
Plasma gun	3 Nylon Brush
Nozzle temperature	10,000 ^{0}C
Current	500 amps
Voltage	65-70 volts
Powder feed	45-50 gms/mint
Spray distance	50 -78 mm

Table 3: Plasma spray parameters for different coating materials

Materials	Primary gas (Argon) Pressure(Bar)	Secondary gas (Hydrogen) Pressure (Bar)	Carrier gas Argon flow (lpm)	Current (amps)	Voltage (volts)	Spray distance (mm)
Al_2O_3+$ZrO_2.5CaO$	3.7	3.45	35	500	65	65-76
Al25Fe7Cr5Ni	6.9	3.30	35	500	65	50-76
$Al_2O_3$30(Ni20Al)	3.7	3.45	35	500	65	65-76

2.3 As-Sprayed Coating Characterization

Scanning electron microscopy (SEM) and X-ray diffractometer (XRD) technique was adopted to do the characterization of the coatings. Primary information viz. coating thickness, micro hardness, porosity, and surface roughness were investigated. The SEM and XRD machine specifications are shown in Table 4 and 5 respectively. The coating error was calculated using empirical relationship and expressed in percent. The micro hardness and porosity analysis were carried out on Clemex CMT, HD model. The Vickers micro hardness was conducted as per ASTM E-384 standard [16], and the test parameters are shown in Table 6. Line intercept method was adopted to determine the average porosity of the coatings. The surface texture of the coated samples was examined using Mitutoyo SJ-210 surface roughness tester as per ISO1997

standard refer Fig.2. The probe travelling speed was maintained at 0.5 mm/s, also some other important specifications of the device are as follows: stylus tip radius: 5µm, detecting measuring force: 4mN, and display type: LCD. On the each sample, 5 trials were done and the average value reported and shown in Table 7.

Fig.2: Mitutoyo SJ-210 surface roughness tester.

Table 4: SEM machine specifications

Parameters for Zeiss Evo 18 special edition	
Filament	Tungsten
Secondary e-image resolution	50 NM
Tilt	0 - 60 Degree
Rotation	360 Degree
EHT	200V - 30KV
Magnification	Up to 50K ~ 100K (depends on sample)

Table 5: XRD Machine Specification

Make	Brukar
Model	D8 Advance
Measuring circle diameter	435,500,600 mm
Smallest addressable increment	0.0001°
Reproducibility	±0.0001°
Anode	Cu, Cr, Co
Detector	Scintillation and Lynxeye

Table 6: Vickers microhardness test parameters

Load	100 g.
Dwell time	10 sec.
Indenter	Diamond pyramid (120°)

3. Instrumentation

3.1 Sample Preparation

In the preparation of wear test samples, the Al-6061 plates were cut into 15mm x 15mm pieces using the isometric cutting tool. These coated pieces were stick to the cylindrical pins using commercially available epoxy resin as shown in Fig.3. Total of 3 specimens were prepared for each coating system, S1, S2, and S3.
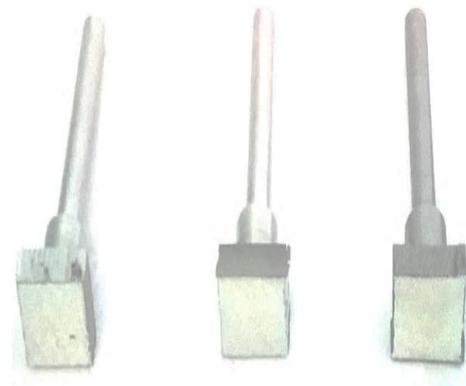
Fig.3: Coated specimens.

3.2 Pin-on-Disk Abrasive Wear Test

The abrasive wear test was carried out on Pin-on–disk tribometer, as per ASTM G132 standard [17]. A commercially available Alumina abrasive disk was used as a counter material whose roughness is determined using Mitutoyo SJ-210. The experimental setup and wear test parameters are shown in Fig. 4 and in Table 7 respectively.

Fig.4: Pin-on-disk tribometer test setup.

Table 7: Abrasive wear test parameters

Rpm	200
Track diameter	80 mm
Load	5,10 & 15 N
Sample size (mm)	15 mm×15 mm
Abrasive disk	Alumina(Ra= 8.51μm)
Test temperature	Room temperature
Rubbing duration	600 sec
Sliding velocity	0.83 m/sec

4. Results and Discussion

4.1 Interpretation on Characterization

The deviation in coating error calculated using an empirical relationship which is as follows: T_{th}-Tact/T_{act}, where T_{th} and T_{act} are theoretical and actual coating thickness respectively and expressed in percentage. The actual coating thickness of the coating systems are shown in Fig.5. The coating error, average surface roughness, average micro hardness, average porosity values for the coating system shown in Table 8. Coating error observed more in case of S1 reason attributed to change in operational parameters viz. feed rate, velocity of impinging jets etc. It has been also observed, as the porosity decreases, hardness proportionally increases, this kind of trend is also observed in other cases [4]. It is also observed in the present coating systems, as the coating thicknesses increases the surface roughness of the top coat also increases. R. G. Bayer et al. [18] had developed an empirical relation between surface roughness and wear and found that wear governed by roughness and the orientation of the asperities. Results obtained in the present case is in agreement with above statement.

XRD analysis carried out with Cu-K-α1 radiation produced at 40 kV and 40mA. The θ-2θ scan was performed between 20º and 89.99º by step width of 0.01036^0.It has been found that phase transformation took place from α- Zirconia dioxide to β- Tazheranite phase within the composite mixture during the plasma coating process. The weight % of β-Tazheranite phase, synthesized from ZrO_2.5CaO found to be 81.08 wt. %. The synthesis of this phase was very novel, and found to minimize the wear mechanism. It is also evident from the XRD pattern [Fig. 6] that sharp peaks and lattice parameters [a=b=c=5.1000, α=β=90º] of composite mixture particles were exist in the cubic crystalline structure with good atomic packing factor. Cubic crystal found offers easy sliding and dislocation as discussed in the forthcoming wear mechanism section [Section 4.2.2].

Table 8: Coating thickness error, surface roughness, hardness, and porosity values of S1, S2& S3 coating system

Coating systems (100μm-S1, 200 μm -S2 & 300 μm -S3)			
	S1	S2	S3
Coating thickness error , %	39.3	4.76	8.1
Average surface roughness, μm	5.90	6.74	7.27
Average hardness, $HV_{0.1}$	442.21	585	616.8
Average porosity, %	1.58	1.41	1.0
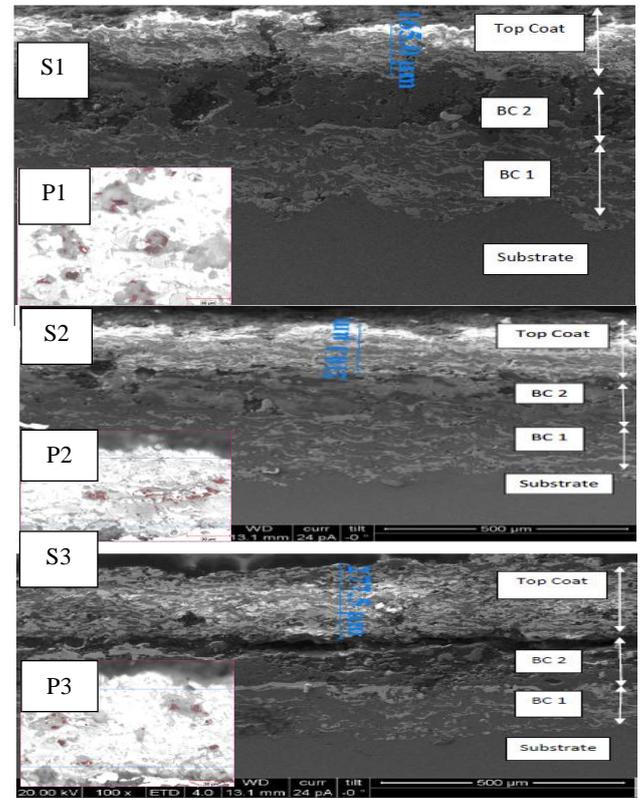
Fig.5: SEM micrograph of S1, S2 & S3 coating thickness and corresponding porosity P1, P2 & P3 of top coat.

4.2 Wear Interpretation

4.2.1 Wear Mechanism of S1, S2, and S3 at 5, 10, & 15 N

The specific wear rates were calculated based on cumulative volume loss/penetration depth of the coating per unit of the applied load and sliding distance [19].The variation of specific wear rate with load ,porosity and hardness is shown in [Fig.10 (g , h, i)]. The cumulative volume loss obtained from the wear versus time data obtained digitally from the computer interfaced with tribometer, and sliding distance was calculated from sliding velocity multiplied with running in time period. It is evident from the graph [Fig. 7 (a, b, c)] that as the load increases wear of the coating increases. The common reason was due to more contact stress established at the interfaces of the asperities at higher load [20]. This can be also understood as follows: Soft phase in the present case zirconia comes under the influence of hard asperities abrasive disk, the soft phase asperities gets squeezed more as the load increases. Mild wear observed between 5 and 10 N normal load and severe wear observed at 15 N load [Fig.7]. Very similar trend of wear was observed from the wear versus time graph with an anomaly at 15 N normal load for S3. Reason of such irregularities can be attributed to the less cohesion between the phases present in the composite mixture and could also acknowledged due to the continuous change in the profile of the asperities of the coating system [21]. It can be also understood as the coating thickness increases exhibit asymptotic behavior [22]. Another interesting phenomenon observed related to coefficient of friction, and it was found that COF value fluctuate in the rage of 0.1 to 0.3 at all the

loading conditions. The reason for constant fluctuation during the running in period could be attributed to continuous deformation and breaking of bonds, and soft phase in contact with the hard protuberances. In the present work it has been observed that friction doesn't depend on the applied loads but primarily depends on the phases and crystallographic crystal structure

4.2.2 Effect of phases and crystalline Structure on Abrasive Wear

Due to anisotropic behavior of ceramic composition, the interpretation of the wear mechanism is a complex task [23]. In this section, an attempt was made to understand the exact mechanism of composite coatings Al_2O_3-ZrO_2·5CaO tested under Alumina abrasive disk. An interesting phenomenon is acknowledged for all the coating systems. The top coat was subjected to more sliding compared to abrasion. The SEM micrograph [Fig.8] along with the enlarged wear versus time graph [Fig. 9] plot clearly shows that the top coat subjected to frequent sliding and wear. Series of stress mark resulted from slip lines refer Fig 8 (S1-5N,) assisted with plastic flow mark refer (S2-5N, S2-15N & S3-10N). Along with localized plowing refer (S2-10N & S3-15N of materials observed more or less same in all the coating systems. This kind of slip lines are also found in many cases of metals and ceramics [24], and localized delamination of the coat [Fig 8: S2-15N, S2-10N] was happened due to less cohesion strength among the constituents. It was evident from the stress pattern and material flow direction that the wear mechanism has mainly governed my slip, and less twinning within the composite mixture. This phenomenon can be understood as follows, within the composite mixture, Tazheranite is a soft phase and it assist in slip of planes. The slip phenomenon principally occurs when slip planes oriented parallel or at right angle to the normal load and hence no plastic deformation [24]. Above investigations also supported by the enlarged wear versus time graph [Fig.9 a,b,c] in all the coating systems. Since all the phases present in the composite mixture found to coexist in the same face centered cubic crystalline structure and the slip has mainly occurs in the plane of <111>,<200>,<220>,<311>,<222>. Also, the topcoat was primary a pure ceramic composition of Al_2O_3-ZrO_2·5CaO the plastic deformation in crystalline ceramics is governed by slip, which finds difficulties due to structural pattern and strong local (electrostatic) potentials [25]. This could also be a probable reason for a very less plastic deformation and more sliding in all the coating system refer Fig.8.The stress mark and wear pattern results on the top surface of the coatings shown in the Fig.8 is in good agreement with the results obtained by Shiv Pratap Singh Yadav et al.[26].The post wear images of samples shown in Fig.11.
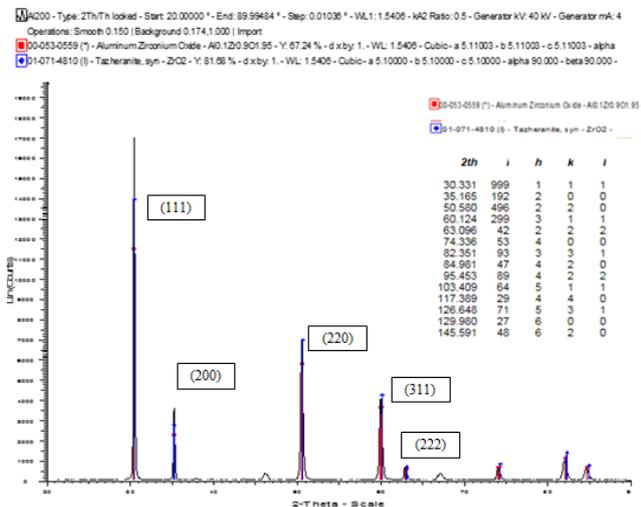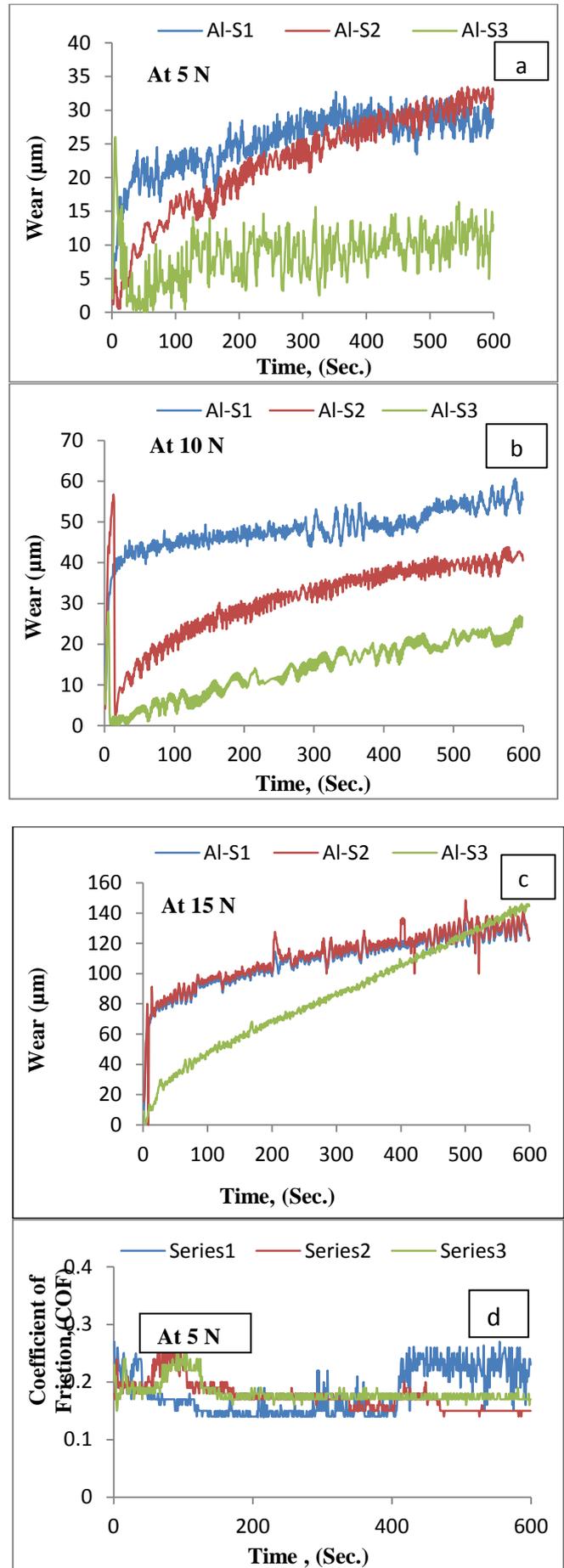
Fig.6: XRD spectrum of Al_2O_3-ZrO_2·5CaO.
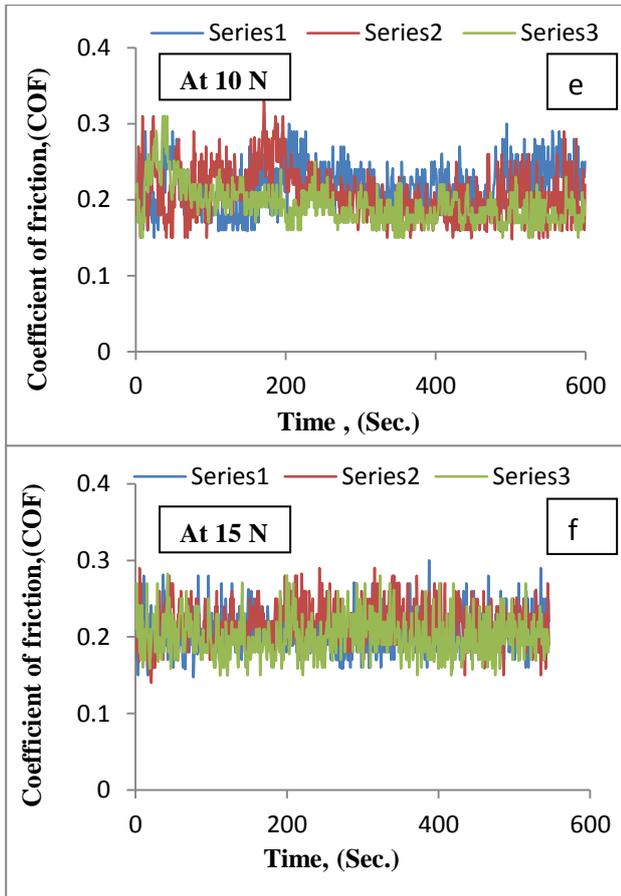
Fig. 7: Wear versus time graph a, b, c, Coefficient of friction versus time graph d ,e, f: at 5,10,15 N normal load.
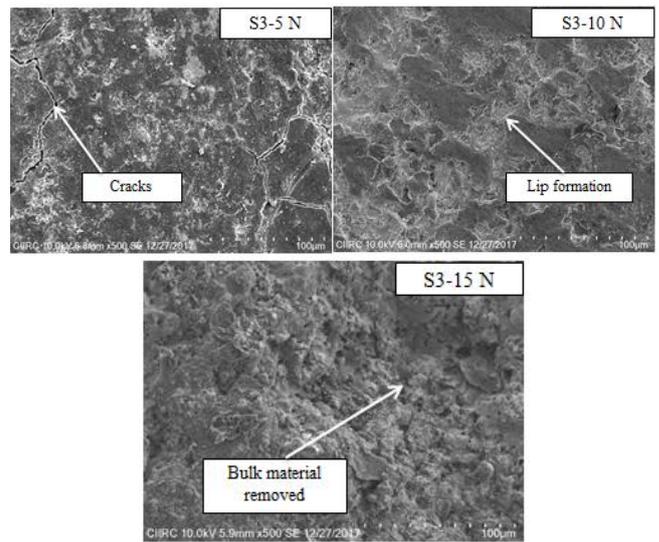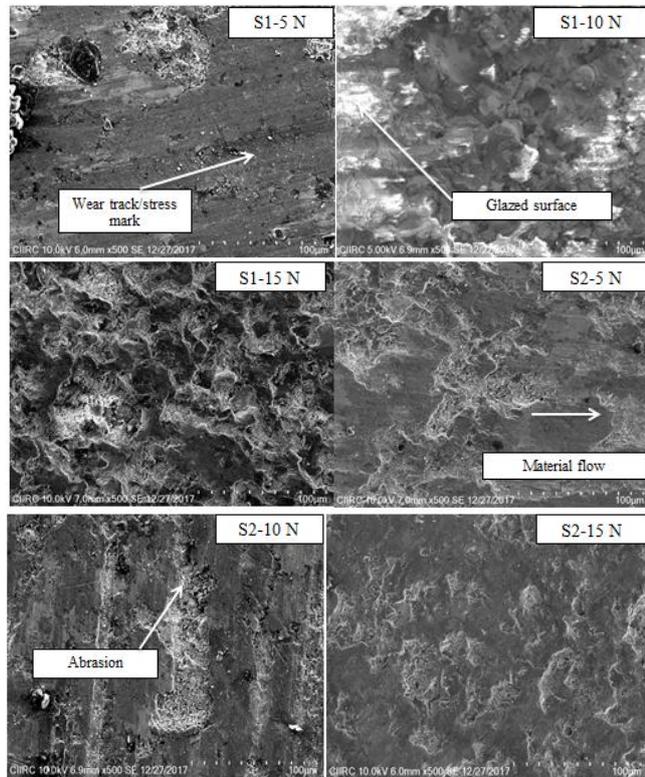
Fig.8: Micrograph of post wear samples S1, S2 and S3 at 5N, 10N and 15 N normal load respectively.
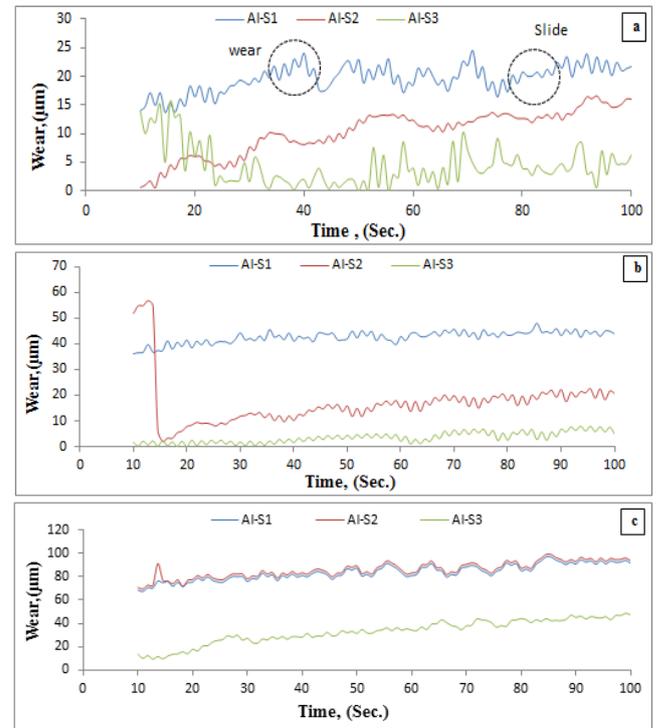
Fig. 9: Enlarged wear versus time graph a, b, & c at 5, 10, 15 N normal load respectively.
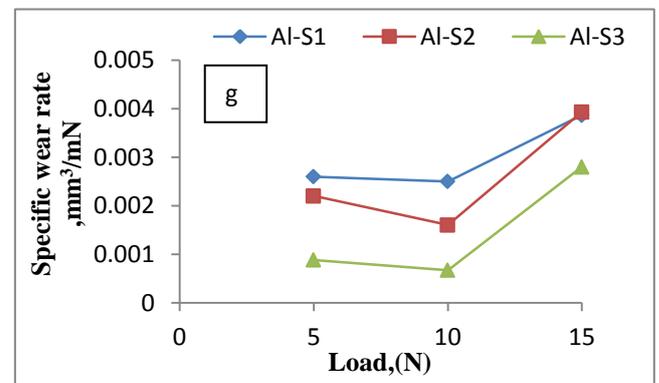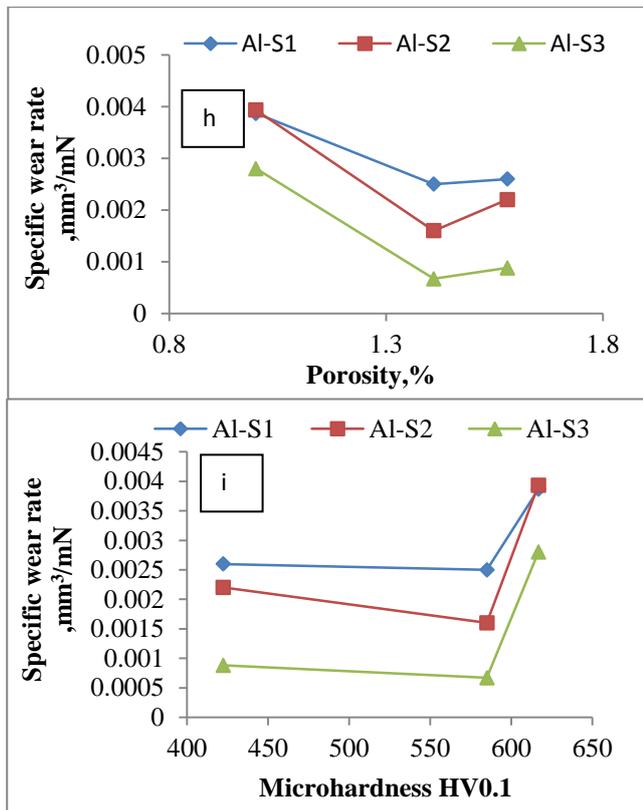
Fig.10: Variation of specific wear rate with d. load e. porosity and f. Microhardness.
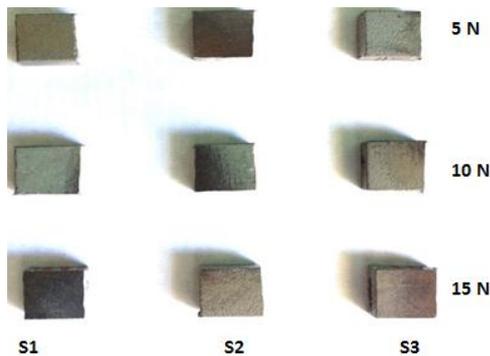
Fig.11: Images of post wear coated samples.

5. Conclusion

An abrasive wear of a composite coatings, alumina and calcia stabilized zirconia (Al_2O_3-ZrO_2.5CaO), blended in 50:50 by wt. % were investigated under abrasive condition at different loading conditions of 5, 10, 15 N in the present investigation. Following are the important conclusions can be drawn from the present tribological studies:

1. The specific wear rate of the coating system demonstrates excellent results within 10 N shadows the effect of normal loads microhardness, and porosity above 10 N normal loads.
2. Coefficient of friction has very little influence and doesn't transcend with the load due to more sliding/slip planes forming face centered cubic crystallographic structure.
3. It was also found that top coat composite mixture was subjected to more sliding and less abrasion. Soft phase being zirconia oxide in the composite mixture offers more sliding and Alumina being hard phase improves hardness and resists abrasion of the coating system. Also, since all the phases present in the composite mixture found to have same symmetrical crystallographic struc-

ture i.e. face centered cubic structure (FCC) also confirmed in XRD analysis, the inter laminar layer shear off very easily irrespective of the applied load.

Future scope of the present study:

An improvement in the present work may be possible by modifying the weight percent of the top coat composite coatings (Al_2O_3+ZrO_2.5CaO) anticipating much greater hardness and improved wear resistance properties.

Acknowledgement

References

[1].Peter A. Engel, Impact Wear of Materials by, Elsevier Scientific Publishing Company, First edition 1976.

[2].Bharat Bhushan, Modern Tribology Handbook, ,Principle of Tribology, CRC Press Volume 1

[3]. P.J. Blau, Friction and Wear Transitions of Materials, Noyes Publications, Park Ridge, NJ, 1989.

[4]. N. Krishnamurthy, M. S. Murali, P. G. Mukunda, M. R.Ramesh, Characterization and wear behavior of plasma-sprayed Al_2O_3 an-$dZrO_2$5CaO coatings on cast iron substrate,J Mater Sci. vol. 45, 2010, pp.850–858.

[5]. N. Krishnamurthy ,M. S. Murali et al.,A Study of Parameters Affecting Wear Resistance of Alumina and Yttria Stabilized Zirconia Composite Coatings on Al-6061 Substrate,International Scholarly Research Network ISRN Ceramics ,2012, pp.1-13

[6]. M.A.Moore, The relationship between the abrasive wear resistance, hardness and microstructure of ferritic materials,Wear, Volume 28, Issue 1, April 1974, pp. 59-68

[7]. G.J.GoreJ.D.Gates, Effect of hardness on three very different forms of wear, Wear ,Volume 203–204, March 1997, pp.544-563.

[8]. I.Sevim, I.B.Eryurek , Effect of fracture toughness on abrasive wear resistance of steels, Materials & Design , Volume27, Issue 10, 2006, pp. 911-919.

[9]. L.Zhou, G.LiuZ.et al., Grain size effect on wear resistanceof a nanostructured AISI52100 Steel, Scripta Materialia,Volume 58, Issue 6, March 2008, pp. 445-448.

[10]. A. V. Makarova, N. N. Soboleva et al., Role of theStrengthening Phases in Abrasive Wear Resistance of Laser-Clad NiCrBSi Coatings, Journal of Friction and Wear,Volume 38, 2017, pp. 272–278.

[11]. H. Liu, M. E. Fine, Modelling of grain size dependent microstructure controlled sliding wear in polycrystalline alumina, J. Am. Ceram. Soc., Volume 76, 1993, pp 2392-2396.

[12]. S.J.Cho, B.J.Hockey, B.R.Lawn, S.J.Bennison, Grain sizeand R-curve effects in the abrasive wear of alumina, J.Am. Ceramic Society, volume 72, 1989, pp. 1249-1252.

[13]. You Wang, Stephen Jiang, Meidong, Shihe Wang,T.Danny Xiao, Peter R. Strutt, Abrasive wear characteristics of plasma sprayed nanostructured alumina/titaniacoatings, Wear 237, 2000, pp 176-185.

[14]. H. K. Xu, S. Jahanmir, J.Mater. Sci, volume 30, 1995, pp2235-2247.

[15]. Abhinav, N.Krishnamurthy et al. Corrosion kinetics ofAl_2O_3+ZrO_2·5CaO coatings applied on gray cast iron substrate, Ceramics International, Volume 43, Issue 17, 1December 2017, pp. 15708-15713.

[16] Vickers microhardness testing, ASTM standard E384,ASTM International, USA.

[17]. ASTM G132 standard, 100 Barr Harbor Drive, WestConshohocken, PA, United States,pp. 19428-2959.

[18] R. G. BAYER et al. The influence of surface roughnesson wear, Wear, 1975, pp. 251 – 260.

[19]. Johnson O. Agunsoye , Talabi S. Isaac et al., Effect ofSilicon Additions on the Wear Properties of Grey CastIron, Journal of Minerals and Materials Characterizationand Engineering, 2013,pp. 61-67.

[20]. P.S.M. Barbour, D.C. Barton et al., The influence of contact stress on the wear of UHMWPE for total replacementhip prostheses, Wear, 1995, pp. 181-183.

[21]. Mechanical Wear Fundamentals and Testing, Revisedand Expanded, By Raymond G. Bayer. CRC press, pp.141.

[22]. I. A. Soldatenkov, A. M. Mezrin et al. Implementation ofAsymptotics of the Wear Contact Problem Solution forIdentifying the Wear Law Based on the Results of Tribological Tests, Journal of Friction and Wear, Volume 38,2017, pp. 173–177

[23]. Donald H. Buckley, Kazuhisa Miyoshi, Friction andwear of ceramics, Wear Volume 100, Issues 1–3, December 1984, pp. 333-353

[24]. Mansur Rastani, Mechanism of slip & twinning, Department of Manufacturing Systems, North Carolina A& TState University 11 1 Price Hall.

[25]. http://www.virginia.edu/bohr/mse209/chapter13.htm

[26]. Shiv Pratap Singh Yadav et al., Abrasive Wear Trends ofNon-Conforming Contact Surfaces, Materials Today:Proceedings 5 (2018), pp.152–160